CHAPTER 3

COSINEOGRAM, A MEASURE OF CIRCULAR-SPATIAL CORRELATION

3.1 Introduction

This chapter defines the cosineogram, which is a graph expressing the empirical correlation of circular-spatial data. The positive definite cosine model with best fit to the cosineogram characterizes the spatial properties of circular-spatial data. This model will be used for circular kriging. Circular kriging (Chapter 4) is the estimation of circular-spatial data based on a model of circular-spatial correlation, which is a function of distance between measurement locations. Cosine models were adapted from three common covariance models from linear kriging (estimation of data of a continuous linear random variable (RV) based on a model of spatial covariance, which is a function of distance between measurement locations).

This chapter is organized as follows: Section 3.2 introduces the cosineogram and model with nugget, range, and sill similar to the nugget, range, and sill of the covariance model used for linear kriging. Section 3.3 derives the result that the theoretical sill is the square of the length of the mean resultant vector of the circular probability distribution underlying the circular-spatial data. Section 3.4 determines that the length of the mean resultant vector is the parameter, ρ, of the circular probability density function (PDF) for the selected circular distributions. Section 3.5 verifies the theoretical sill by simulation. Section 3.6 defines some cosine models (similar to covariance models used for linear kriging) for fitting to a cosineogram. Section 3.7 constructs an example cosineogram for ocean wind in a south polar region. Section 3.8 concludes with the summary and future work.

3.2 The Cosineogram

Circular-spatial data may have an underlying spatial trend where the mean direction depends on location. The random component of direction contains information about the spatial correlation. The empirical cosineogram is defined as the plot of the mean cosine of the angular distance (Figure 3-1, right) between the random components of direction vs. the Euclidean or linear distance between observation locations (Figure 3-1, left).

Let $\hat{\varsigma}(d)$ be the estimate of the mean cosine, which depends on the Euclidean distance d between measurement locations, $\boldsymbol{x}_i$ and $\boldsymbol{x}_j$ vectors of location coordinates of observations i and j, respectively, $\| \boldsymbol{x}_j - \boldsymbol{x}_i \|$ the Euclidean distance between observation locations, $N(d)$ the number of pairs of observations separated by a distance $\| \boldsymbol{x}_j - \boldsymbol{x}_i \|$ within a tolerance ε of d, and θ_i and θ_j the measured directions at $\boldsymbol{x}_i$ and $\boldsymbol{x}_j$, respectively. The cosineogram is the plot of $\hat{\varsigma}(d) = \left(1/N(d)\right) \sum_{\left| \| \boldsymbol{x}_j - \boldsymbol{x}_i \| - d \right| < \varepsilon} \cos\left(\theta_j - \theta_i\right)$ vs. d. The cosine model of spatial correlation underlying the sampling variation in the cosineogram are illustrated by Figure 3-2.

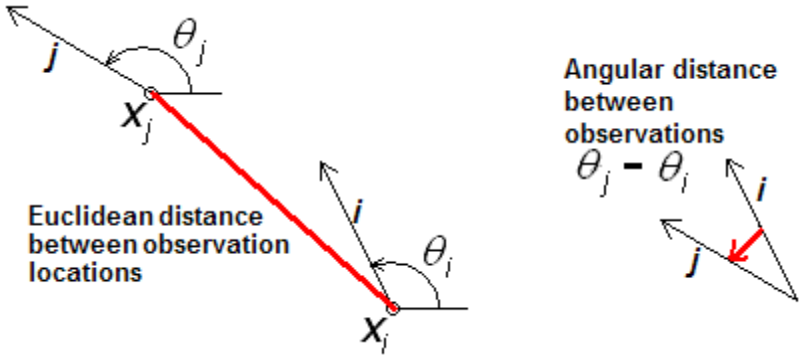

Figure 3-1. Euclidean Distance Between Locations vs. Angular Distance Between Observations. Euclidean and angular distances between observations are indicated by red lines.

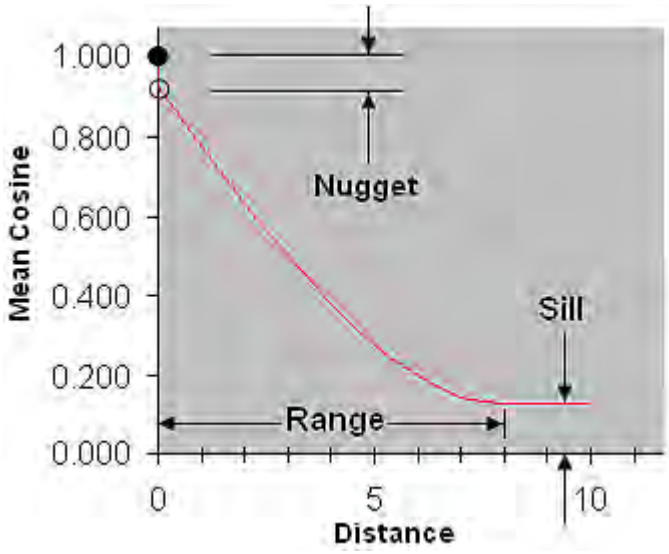

Figure 3-2. Features of the Cosine Model. The cosineogram characterizes the correlation of random components of direction vs. distance between locations. For the spherical cosine model, the sill is flat at distances beyond the range.

The value of the mean cosine of the angle between observations at zero distance is defined to be one because the angle between an observation and the same observation at the same location is zero. Measurement error may cause observations at locations which are close together (or even at the same location) to be more variable resulting in a decrease in the mean cosine. The difference between 1.0 and the mean cosine at distances approximately zero is called the nugget. As the distance between measurement locations increases, the nonrandom or spatial trend component of direction may change, and the random component of direction will have less correlation resulting in a decrease of the mean cosine of the random components of direction. For the spherical model shown in Figure 3-2, the range is defined as the distance at which the random components are no longer correlated. For other models, the practical range, which is a multiple of the range, is the distance at which random components are assumed to be uncorrelated. At distances where observations of direction are uncorrelated, the mean cosine is a constant, forming a plateau which is called the sill.

The next section will derive the result that the theoretical sill is the square of the resultant vector mean length parameter (Chapter 1, Section 1.1) of the circular distribution of the CRF (Chapter 1, Section 1.1). It is based on the new definition that the theoretical sill of the CRF is the expectation of the cosines of the small angles between pairs of independent CRVs. This definition parallels the definition of the sill of a covariogram in linear kriging. The covariogram is a plot of the empirical covariance vs. distance between observation locations. At distances where linear RVs are uncorrelated, the covariance is zero, forming a sill in the covariogram.

3.3 Derivation of the Sill

3.3.1 Review of Circular Probability Distributions and Statistics

A circular random variable (CRV) takes random directions with the total probability of all possible directions distributed on the circular support. In this chapter, direction will be expressed in radian units on the support $[0,2\pi)$ since trigonometric functions require angles in radian units. To determine the properties of a circular probability distribution, imagine a point on a unit circle plotting a direction as the equivalent unit vector located at the origin of the unit circle with arrow head touching the unit circle. The main properties of a circular probability distribution include the resultant vector mean direction μ, which may depend on measurement location, and the resultant vector mean length ρ, which is a measure of concentration about the resultant vector mean direction and the opposite of variability about the mean, which is a measure of spread.

Let a vector be denoted by a bold lower case letter and a scalar by a nonbolded lower case letter. Let $\theta_1, \theta_2, \cdots, \theta_n$ be a set of n observations of the corresponding CRVs

$\Theta_1, \Theta_2, \cdots, \Theta_n$ measured in radians. With $C_n = \sum_{i=1}^{n} \cos\theta_i$ and $S_n = \sum_{i=1}^{n} \sin\theta_i$, the sample mean resultant vector direction $\bar{\theta}$ is

$$\bar{\theta} = \begin{cases} \tan^{-1}(v/h), & h > 0, v \geq 0 \\ \pi/2, & h = 0, v > 0 \\ \tan^{-1}(v/h) + \pi, & h < 0 \\ \frac{3}{2}\pi, & h = 0, v < 0 \\ \tan^{-1}(v/h) + 2\pi, & h > 0, v < 0 \\ \text{undefined}, & h = v = 0. \end{cases} \tag{3.1}$$

The population resultant vector mean direction is denoted by μ.

In terms of C_n and S_n, the sample resultant vector length is

$$R_n = \sqrt{C_n^2 + S_n^2}, \tag{3.2}$$

and the sample resultant vector mean length is

$$\bar{R}_n = \tfrac{1}{n} R_n. \tag{3.3}$$

If all n observations have the same direction, the variability is zero, the resultant vector length $R_n = n$ (the unit vector observations of direction added tail to head are aligned and n long), and the resultant vector mean length $\bar{R}_n = \tfrac{1}{n} n = 1$, which is the theoretical maximum. When direction takes random values, the variability is greater than 0, the resultant vector length $R_n < n$, and $\bar{R}_n = \frac{1}{n} R_n < 1$. If n is even, and the angles between all pairs of adjacent observations of direction are equal, the variability (spread) is the theoretical maximum, the horizontal and vertical components of the unit vectors cancel, $R_n = 0$, $\bar{R}_n = \frac{1}{n} R_n = 0$, and the resultant vector mean direction $\bar{\theta}_n$ is undefined.

The population mean resultant vector length is denoted by ρ. The circular distributions discussed in this dissertation were introduced in Chapter 1, Section 1.1, and are characterized in Table 3-1.

Table 3-1. Circular Probability Distributions, $\mu = 0,\ 0 \le \theta < 2\pi$ Radians. Circular density is plotted as the length of radial between black filled unit circle and outer curve.

Name of Distribution	Circular PDF Plot	Circular PDF Function	Range of Parameter	Value of ρ in PDF Plot
Cardioid	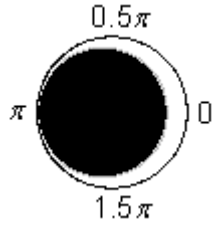	$\frac{1}{2\pi}\left[1+2\rho\cos(\theta)\right]$	$0 < \rho \le 0.5$	$\rho =$ 0.95 x 0.5
Triangular	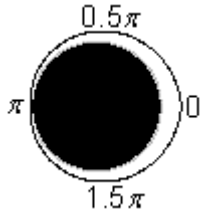	$\frac{4-\pi^2\rho+2\pi\rho\lvert\pi-\theta\rvert}{8\pi}$	$0 < \rho \le \frac{4}{\pi^2}$	$\rho = .95 \times \frac{4}{\pi^2}$
Uniform	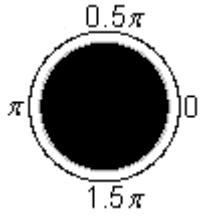	$\frac{1}{2\pi}$	NA	NA
von Mises	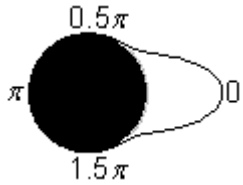	$\frac{\exp(\kappa\cos(\theta))}{2\pi\sum_{j=0}^{\infty}\left(\frac{\kappa}{2}\right)^{2j}\left(\frac{1}{j!}\right)^2}$	$0 < \kappa < \infty$	$\kappa = 10.2696$ equivalent to $\rho = .95$
Wrapped Cauchy	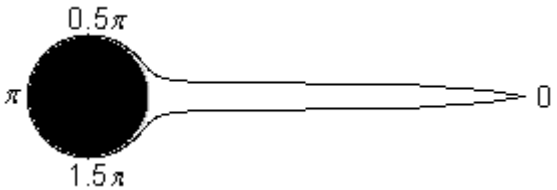	$\frac{1}{2\pi}\frac{1-\rho^2}{1+\rho^2-2\rho\cos(\theta)}$	$0 < \rho < 1$	$\rho =$ 0.95 x 1

3.3.2 Assumptions

The dimension of the stochastic space is 2. The circular-spatial model consists of a spatial trend, with mean direction dependent on location or constant, plus a circular random field (CRF). With Θ the CRV and $\boldsymbol{x}$ the location in R^2, the CRF is the set $\{\Theta(\boldsymbol{x}), \boldsymbol{x} \in R^2\}$.

Spatial correlation increases as distance between measurement locations decreases, i.e., random components of direction (spatial trend removed) tend to be more similar as distance between observation locations decreases. In the form required by the circular kriging of Chapter 4, spatial correlation is the mean cosine of the angle between random components of directions vs. distance between observation locations. It is assumed that the spatial correlation is isotropic, i.e., it is independent of the geographic direction in which sampling is performed. If the spatial correlation varied with geographic direction (anisotropic) and sampling was performed in directions with different spatial correlation, the estimate of spatial correlation (mean cosine vs. distance) would be some average over geographic directions, and less accurate for a particular direction. Geometric anisotropy, where the sill is constant and the range varies with the spatial direction in which observations are taken, requires a directional cosineogram (mean cosine computed within a tolerance of a specified geographic direction) and applies to the geographic area over which the directional cosineogram is computed .

3.3.3 The Sill a Function of Expectations

Let Θ be the CRV of the circular distribution, Θ_i and Θ_j be two random directions, $0 \le \Theta_i, \Theta_j < 2\pi$, with equivalent unit vector denoted by $\boldsymbol{i}$ and $\boldsymbol{j}$. Also, let E be the expectation operator, and D be the smallest angle in radians between two independent random directions of a circular probability distribution, $0 \le D \le \pi$. Define the

sill as the $E\{\cos(D)\}$. The sill will be derived for the cases shown in Figure 3-3.

Either $0 \le |\Theta_j - \Theta_i| < \pi$ (Case 1), or $\pi \le |\Theta_j - \Theta_i| < 2\pi$ (Case 2).

Case 1, $0 \le |\Theta_j - \Theta_i| < \pi$:

$$
\begin{aligned}
E\{\cos(D)\} &= E\{\cos|\Theta_j - \Theta_i|\} \\
&= \begin{cases} E\{\cos(\Theta_j - \Theta_i)\}, \Theta_j \ge \Theta_i \\ E\{\cos[-(\Theta_j - \Theta_i)]\}, \Theta_j < \Theta_i \end{cases} \\
&\overset{\cos(\alpha)=\cos(-\alpha)}{=} E\{\cos(\Theta_j - \Theta_i)\} \\
&\overset{\text{TRIG IDENTITY}}{=} E\{\cos(\Theta_j)\cos(\Theta_i) + \sin(\Theta_j)\sin(\Theta_i)\} \\
&= E\{\cos(\Theta_j)\cos(\Theta_i)\} + E\{\sin(\Theta_j)\sin(\Theta_i)\} \\
&\overset{iid}{=} E\{\cos(\Theta)\}E\{\cos(\Theta)\} + E\{\sin(\Theta)\}E\{\sin(\Theta)\} \\
&= [E\{\cos(\Theta)\}]^2 + [E\{\sin(\Theta)\}]^2
\end{aligned}
$$

Case 2, $\pi \le |\Theta_j - \Theta_i| < 2\pi$:

$$
\begin{aligned}
E\{\cos(D)\} &= E\{\cos(2\pi - |\Theta_j - \Theta_i|)\} \\
&= E\{\cos(2\pi)\cos|\Theta_j - \Theta_i| + \sin(2\pi)\sin|\Theta_j - \Theta_i|\} \\
&= E\{\cos|\Theta_j - \Theta_i|\} \\
&\overset{\text{above}}{=} [E\{\cos(\Theta)\}]^2 + [E\{\sin(\Theta)\}]^2
\end{aligned}
$$

$$
\Rightarrow E\{\cos(D)\} = [E\{\cos(\Theta)\}]^2 + [E\{\sin(\Theta)\}]^2 \qquad (3.4)
$$

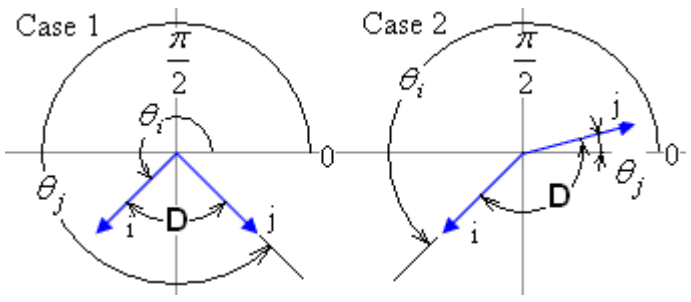

Figure 3-3. Cases of Random Directions. Directions are expressed in radian units.

Hence, complete evaluation of the sill requires knowledge of $E\{\cos(\Theta)\}$ and $E\{\sin(\Theta)\}$.

3.3.4 Expectation of the Sines

With *g* the PDF of Θ, for the symmetric circular distributions with $\mu = 0$, the PDF $g(\theta) = g(-\theta)$. Hence, the oppositely signed $\sin(\Theta)$ and $\sin(-\Theta)$ cancel when integrating over the full range and, hence, $E\{\sin(\Theta)\} = 0$ for $\mu = 0$. Let $\tilde{\rho}$ be the population mean resultant vector length. $E\{\sin(\Theta)\} = 0$ for $\mu = 0$, i.e., the vertical component of $\tilde{\rho}$ is zero. Hence

$$\tilde{\rho} = E\{\cos(\Theta)\}. \tag{3.5}$$

3.4 Expectation of the Cosines

From (3.5), the population mean resultant vector length $\tilde{\rho} = E\{\cos(\Theta)\}$ for $\mu = 0$. To evaluate $E\{\cos(\Theta)\}$, the PDFs for circular distributions summarized in Table 3-1 were obtained from Mardia (1972), Fisher (1993), and Jammalamadaka and SenGupta (2001). In the subsections 3.4.1 to 3.4.5, it will be shown that $\tilde{\rho}$ is the parameter ρ of the circular PDFs for the selected circular probability distributions. This step is necessary as it is not immediately obvious that the parameter ρ is the population mean resultant vector length for the selected distributions, as claimed by Fisher (1993).

3.4.1 Cardioid

$$E\{\cos(\Theta)\,|\,\text{Cardioid}\} = \int_0^{2\pi} \cos(\theta) \underbrace{\left(\frac{1}{2\pi}[1+2\rho\cos(\theta)]\right)}_{\text{DENSITY}} d\theta$$

$$= \frac{1}{2\pi}\int_0^{2\pi} \left(\cos(\theta) + 2\rho\cos^2\theta\right) d\theta$$

$$= \frac{1}{2\pi}\int_0^{2\pi} \cos(\theta)\, d\theta + \frac{1}{2\pi}\int_0^{2\pi} 2\rho\cos^2\theta\, d\theta$$

$$= \frac{1}{2\pi}\sin(\theta)\Big|_0^{2\pi} + \frac{1}{\pi}\int_0^{2\pi} \rho\cos^2\theta\, d\theta$$

$$= 0 + \frac{\rho}{\pi}\int_0^{2\pi} \frac{1+\cos(2\theta)}{2}\, d\theta$$

$$= \frac{\rho}{2\pi}\int_0^{2\pi} 1\, d\theta + \frac{\rho}{2\pi}\int_0^{2\pi} \cos(2\theta)\, d\theta$$

$$= \frac{\rho}{2\pi}\theta\Big|_0^{2\pi} + \frac{1}{2}\frac{\rho}{2\pi}\int_0^{2\pi} \cos(2\theta)\, 2d\theta$$

$$= \frac{\rho}{2\pi}2\pi + \frac{\rho}{4\pi}\sin(2\theta)\Big|_0^{2\pi}$$

$$= \rho + \frac{\rho}{4\pi}\sin(0)$$

$$= \rho \Rightarrow$$

$$E\{\cos(\Theta)\,|\,\text{Cardioid}\} = \rho \tag{3.6}$$

3.4.2 Triangular

$$E\{\cos(\Theta)\,|\,\text{Triangular}\} = \int_0^{2\pi} \cos(\theta) \underbrace{\frac{1}{8\pi}\left(4 - \pi^2\rho + 2\pi\rho\,|\,\pi - \theta|\right)}_{\text{DENSITY}} d\theta$$

$$= \frac{1}{8\pi}\int_0^{2\pi} \cos(\theta)\left(4 - \pi^2\rho\right) d\theta + \frac{1}{8\pi}\int_0^{2\pi} \cos(\theta) 2\pi\rho\,|\pi - \theta|\, d\theta$$

$$= \frac{\left(4 - \pi^2\rho\right)}{8\pi}\sin(\theta)\Big|_0^{2\pi} + 2\pi\rho\frac{1}{8\pi}\int_0^{\pi} \cos(\theta)(\pi - \theta)\, d\theta$$

$$+ 2\pi\rho\frac{1}{8\pi}\int_{\pi}^{2\pi} \cos(\theta)(\theta - \pi)\, d\theta$$

$$= 0 + 2\pi\rho\frac{\pi}{8\pi}\int_0^{\pi} \cos(\theta)\, d\theta - 2\pi\rho\frac{1}{8\pi}\int_0^{\pi} \theta\cos(\theta)\, d\theta$$

$$- 2\pi\rho\frac{\pi}{8\pi}\int_{\pi}^{2\pi} \cos(\theta)\, d\theta + 2\pi\rho\frac{1}{8\pi}\int_{\pi}^{2\pi} \theta\cos(\theta)\, d\theta$$

$$
\begin{aligned}
&= \frac{\pi\rho}{4}\int_0^{\pi}\cos(\theta)\,d\theta - \frac{\rho}{4}\int_0^{\pi}\theta\cos(\theta)\,d\theta - \frac{\pi\rho}{4}\int_{\pi}^{2\pi}\cos(\theta)\,d\theta \\
&\quad + \frac{\rho}{4}\int_{\pi}^{2\pi}\theta\cos(\theta)\,d\theta \\
&= \frac{\pi\rho}{4}\sin(\theta)\Big|_0^{\pi} - \frac{\rho}{4}\{\cos(\theta)+\theta\sin(\theta)\}\Big|_0^{\pi} \\
&\quad - \frac{\pi\rho}{4}\sin(\theta)\Big|_{\pi}^{2\pi} + \frac{\rho}{4}\{\cos(\theta)+\theta\sin(\theta)\}\Big|_{\pi}^{2\pi} \\
&= 0 - \frac{\rho}{4}\{-1-1+0\} - 0 + \frac{\rho}{4}\{1--1+0\} \\
&= -\frac{\rho}{4}\{-2\} + \frac{\rho}{4}\{2\} \\
&= \frac{\rho}{2} + \frac{\rho}{2} \\
&= \rho \Rightarrow
\end{aligned}
$$

$$E\{\cos(\Theta)\,|\,\text{Triangular}\} = \rho \tag{3.7}$$

3.4.3 Uniform

$$
\begin{aligned}
E\{\cos(\Theta)\,|\,\text{Uniform}\} &= \int_0^{2\pi}\cos(\theta)\underbrace{[2\pi]^{-1}}_{\text{DENSITY}}d\theta = \\
&= \frac{1}{2\pi}\sin(\theta)\Big|_0^{2\pi} \\
&= 0 \\
&\overset{\rho\equiv 0}{=} \rho \Rightarrow
\end{aligned}
$$

$$E\{\cos(\Theta)\,|\,\text{Uniform}\} = \rho \tag{3.8}$$

3.4.4 von Mises

With $I_0(\kappa) = \frac{1}{2\pi}\int_0^{2\pi}\exp(\kappa\cos(\theta))\,d\theta$ and $I_1(\kappa) = \frac{1}{2\pi}\int_0^{2\pi}\cos(\theta)\exp(\kappa\cos(\theta))\,d\theta$

(Jammalamadaka and SenGupta 2001, p. 288), $A_1(\kappa) = \frac{I_1(\kappa)}{I_0(\kappa)}$ (Fisher 1993, p. 50, eq. 3.36).

$$E\{\cos(\Theta)\,|\,\text{von Mises}\} = \int_0^{2\pi} \cos(\theta) \underbrace{\frac{1}{2\pi\, I_0(\kappa)} \exp(\kappa\cos(\theta))}_{\text{DENSITY}}\, d\theta$$

$$= \frac{1}{I_0(\kappa)} \frac{1}{2\pi} \int_0^{2\pi} \cos(\theta)\exp(\kappa\cos(\theta))\, d\theta$$

$$= \frac{1}{I_0(\kappa)} I_1(\kappa)$$

$$= A_1(\kappa)$$

$$\overset{\text{(Fisher 1993, p. 49)}}{=} \qquad \rho \Rightarrow$$

$$E\{\cos(\Theta)\,|\,\text{von Mises}\} = \rho \tag{3.9}$$

3.4.5 Wrapped Cauchy

Jammalamadaka and SenGupta (2001, p. 45) prove the equivalence of the PDF from Table 3-1 and the form of the PDF used below.

$$E\{\cos(\Theta)\,|\text{WrCauchy}\} = \int_0^{2\pi} \cos(\theta) \underbrace{\frac{1}{2\pi}\left[1 + 2\sum_{k=1}^{\infty} \rho^k \cos(k\theta)\right]}_{\text{DENSITY}} d\theta$$

$$= \frac{1}{2\pi} \int_0^{2\pi} \left[\cos(\theta) + 2\sum_{k=1}^{\infty} \rho^k \cos(\theta)\cos(k\theta)\right] d\theta$$

$$= \frac{1}{2\pi} \int_0^{2\pi} \cos(\theta)\, d\theta + \frac{1}{2\pi} \int_0^{2\pi} 2\sum_{k=1}^{\infty} \rho^k \cos(\theta)\cos(k\theta)\, d\theta$$

$$= \frac{1}{2\pi} \sin(\theta)\Big|_0^{2\pi} + \frac{1}{\pi} \sum_{k=1}^{\infty} \rho^k \int_0^{2\pi} \cos(\theta)\cos(k\theta)\, d\theta$$

$$= 0 + \frac{1}{\pi} \rho^1 \int_0^{2\pi} \cos(\theta)\cos(\theta)\, d\theta + \frac{1}{\pi} \sum_{k=2}^{\infty} \rho^k \int_0^{2\pi} \cos(\theta)\cos(k\theta)\, d\theta$$

$$= \frac{1}{\pi} \rho \left[\underbrace{.5\sin(\theta)\cos(\theta) + .5\theta}_{\text{Weast 1972, p. A-136, \#302}} \right]_0^{2\pi}$$

$$+ \frac{1}{\pi} \sum_{k=2}^{\infty} \rho^k \left[\underbrace{\frac{1}{2(k-1)} \sin(\theta(k-1)) + \frac{1}{2(k+1)} \sin(\theta(k+1))}_{\text{Weast 1972, p. A-137, \#317}} \right]_0^{2\pi}$$

$$= \frac{1}{\pi} \rho [0 - 0 + \pi - 0] + \frac{1}{\pi} \sum_{k=2}^{\infty} \rho^k [0 - 0 + 0 - 0]$$

$$= \frac{1}{\pi} \rho\pi + \frac{1}{\pi} \sum_{k=2}^{\infty} 0 = \rho \Rightarrow$$

$$E\{\cos(\Theta)\,|\,\text{WrCauchy}\} = \rho \tag{3.10}$$

3.4.6 Summary of Individual Results

In summary, from (3.6) to (3.10) for the selected distributions from Table 3-1, the population mean resultant vector length $\tilde{\rho}$ equals the parameter ρ of the circular probability distribution. Let the parameter ρ also denote the mean resultant vector length. Hence, the theoretical sill is

$$E\{\cos(D)\} = \rho^2. \tag{3.11}$$

Result (3.11) has two implications. First, two circular distributions of different families (Cardioid, Triangular, von Mises, Wrapped Cauchy) with the same population mean resultant vector length, ρ, will have the same theoretical sill, ρ^2. Hence, with the exception of the uniform circular distribution, the correspondence between the sill and a circular probability distribution is not unique. For the uniform circular distribution, $\rho = 0$ because all directions have equal probability density. The second implication is that zonal anisotropy (sill varies with direction) cannot occur in a pure CRF with one underlying circular probability distribution.

3.5 Verification of the Sill by Simulation

The theoretical sill was computed as ρ^2 for five circular probability distributions from Table 3-1. The results have been summarized in Table 3-2. The function A_1 in the Sill column of the table for the von Mises distribution is given in Subsection 3.4.4. The value of the sill of each distribution was verified by simulation.

Figures 3-4 to 3-8 were computed using the R code in Appendices K.3 and L.1. For each distribution, 1000 simulations were computed. In each simulation, 100 independent CRV were computed, the cosines of the angles between all pairs of CRV were collected, and the averages were computed for the cumulative collection of

Table 3-2. The Sill of Selected Distributions.

Distribution	Parameter Range	Selected Parameter Value	Sill, or $E\{\cos(D)\} = \rho^2$ (3.11)
Cardioid	$0 < \rho \le 0.5$	$\rho = 0.25$	$\rho^2 = 0.25^2 = 0.062$
Triangular	$0 < \rho \le 4/\pi^2$	$\rho = 2/\pi^2$	$\rho^2 = \left(2/\pi^2\right)^2 = 0.041$
Uniform	$\rho = 0$	$\rho = 0$	$\rho^2 = 0$
von Mises	$0 < \kappa < \infty$ $(0 < \rho < 1)$	$\kappa = 5$ (concentration)	$\rho^2 = (A_1(5))^2 = 0.798$
Wrapped Cauchy	$0 < \rho < 1$	$\rho = \exp(-1)$	$\rho^2 = (\exp(-1))^2 = 0.135$

cosines. Hence, the size of the collection increases with each simulation. Figures 3-4 to 3-8 plot the mean cosine of the angle between independent CRV vs. the number of simulations, and show that the mean cosine tends to the theoretical sill as the number of simulations increases and is consistent with the theoretical sill. In Figure 3-6, a slightly negative mean cosine developed at about 200 simulations. After 300 simulations, the mean cosine trended toward zero. With the uniform circular distribution all directions are equally likely. Hence, half of the angles are likely to occur between 0.5π and 1.5π. These have negative cosines. A negative mean cosine means there were more negative than positive cosines at the completion of a simulation in the sequence of simulations.

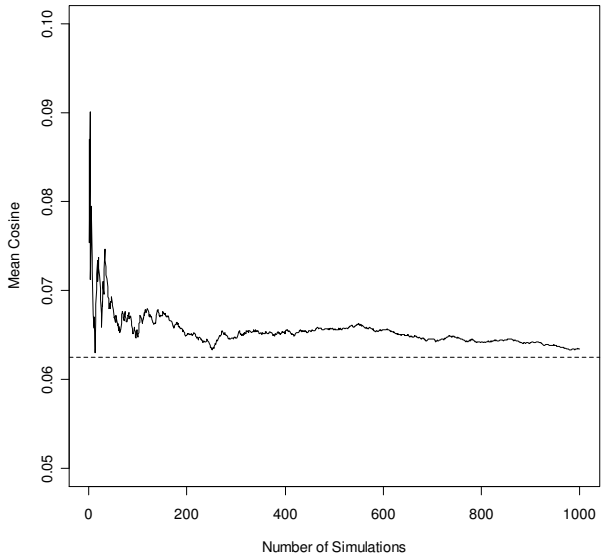

Figure 3-4. Mean Cosine of the Angle Between Independent Cardioid CRV, $\rho^2 = 0.062$, Is Consistent with the Theoretical Sill. The dashed line represents the theoretical sill.

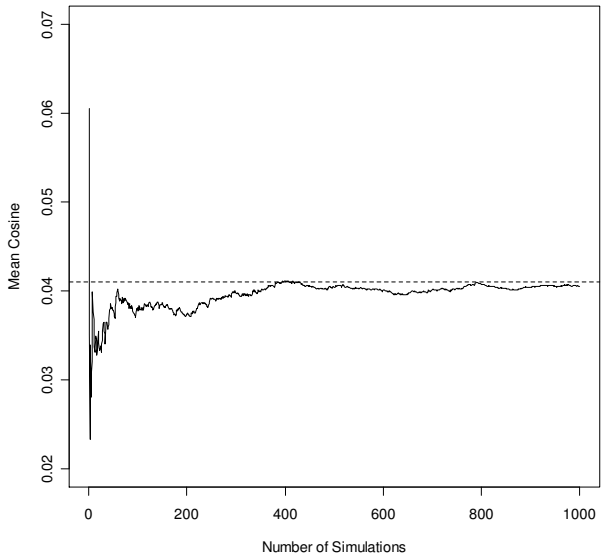

Figure 3-5. Mean Cosine of the Angle Between Independent Triangular CRV, $\rho^2 = 0.041$, Is Consistent with the Theoretical Sill. The dashed line represents the theoretical sill.

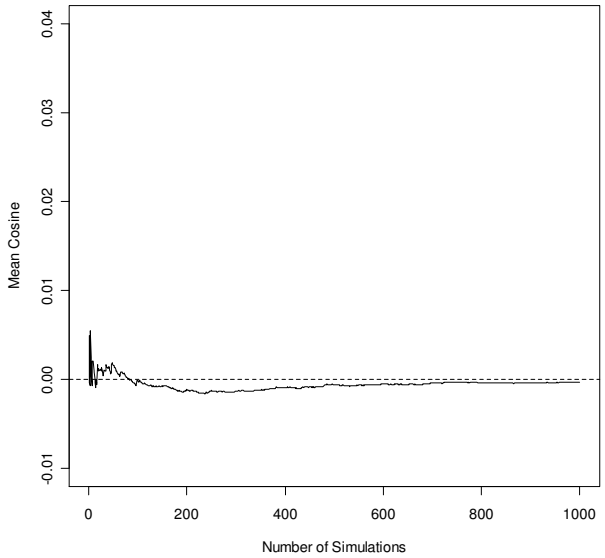

Figure 3-6. Mean Cosine of the Angle Between Independent Uniform CRV, $\rho^2 = 0$, Is Consistent with the Theoretical Sill. The dashed line represents the theoretical sill.

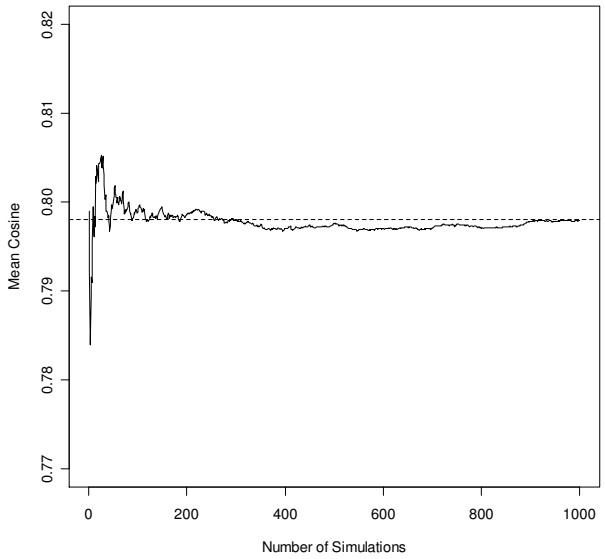

Figure 3-7. Mean Cosine of the Angle Between Independent von Mises CRV, $\rho^2 = 0.798$, Is Consistent with the Theoretical Sill. The dashed line represents the theoretical sill.

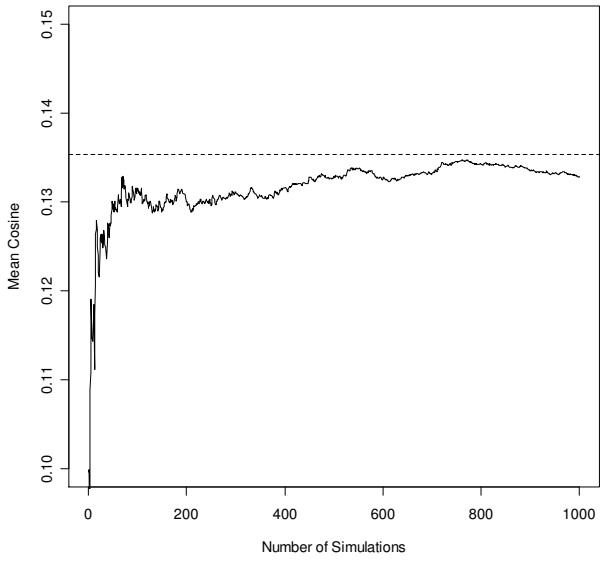

Figure 3-8. Mean Cosine of the Angle Between Independent Wrapped Cauchy CRV, $\rho^2 = 0.135$, Is Consistent with the Theoretical Sill. The dashed line represents the theoretical sill.

3.6 Cosine Models

3.6.1 Cosine Model Properties

In the previous sections, the mean cosine of the angle between independent CRV was determined to be ρ^2. We now will consider the CRF. Covariance models used for linear kriging were derived from the semivariance models in Bailey and Gatrell (1995, pp. 179-180). These covariance models are monotonic decreasing and positive definite. Cosine models were adapted from covariance models by scaling and shifting to conform to the circular-spatial correlation in a CRF:

- At distance 0, the mean cosine equals 1.
- At distance not exactly 0, but close to 0, the mean cosine equals 1 minus the nugget.
- As distance increases, the mean cosine decreases monotonically to the sill.
- The sill equals the square of the mean resultant vector length parameter ρ of the circular probability distribution.

- Applying the cosine model to the matrix of pairwise distances produces a symmetric and positive definite matrix, which will be proved. A positive definite matrix is required for linear kriging.

3.6.2 Introductory Cosine Models Adapted from Linear Kriging

Let ρ be the mean resultant vector length of the circular probability distribution, $0 \le \rho < 1$, and n_g be the nugget. Since the minimum value of the mean cosine is ρ^2, the maximum nugget (Figure 3-2) is $1-\rho^2$. Hence, $0 \le n_g < 1-\rho^2$. With $\varsigma(d)$ the mean cosine of the angle between random components of direction a distance *d* apart and *r* the range, some introductory cosine models adapted from Bailey and Gatrell (1995, pp. 179-180) by scaling and shifting, are:

- The Exponential Cosine Model

$$\varsigma(d) = \begin{cases} 1, d = 0 \\ \rho^2 + (1 - n_g - \rho^2)\exp(-3\,d/r), d > 0 \end{cases} \tag{3.12}$$

- The Gaussian Cosine Model

$$\varsigma(d) = \begin{cases} 1, d = 0 \\ \rho^2 + (1 - n_g - \rho^2)\exp\left(-3\,[d/r]^2\right), d > 0 \end{cases} \tag{3.13}$$

- The Spherical Cosine Model

$$\varsigma(d) = \begin{cases} 1, d = 0 \\ 1 - n_g - (1 - n_g - \rho^2)\left(\frac{3}{2}[d/r] - \frac{1}{2}[d/r]^3\right), \quad 0 < d \le r \\ \rho^2, \quad d > r. \end{cases} \tag{3.14}$$

Note that the symbol $\hat{\varsigma}(d)$ is used for the empirical version of the model, which is the cosineogram (Section 3.2).

Figures 3-9 to 3-11 show plots of cosine models for the selected circular distributions with range $r = 8$ and nugget $n_g = 0$. Values for the parameters ρ and κ have been chosen in accordance with Table 3-2 and with Figures 3-4 to 3-8. The parameter κ of the von Mises (vM) distribution is a measure of concentration about the mean direction equal to one half the log of the ratio of the maximum density at the mean to the minimum density at the opposite direction. The exponential model in Figure 3-9 is concave up, the Gaussian model in Figure 3-10 is "S" shaped with an inflexion point, and the spherical model in Figure 3-11 has a plateau (sill) at distances beyond the range. Additional suitable cosine models are given in Appendix M.

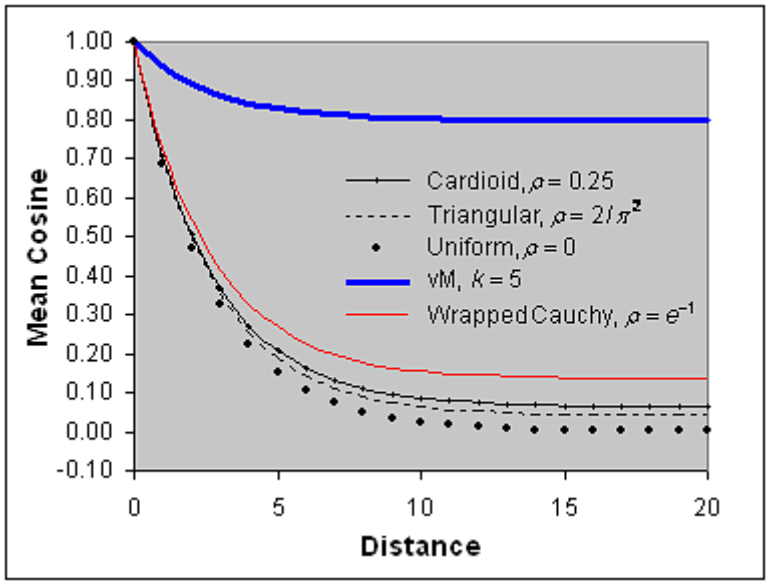

Figure 3-9. The Exponential Cosine Model.

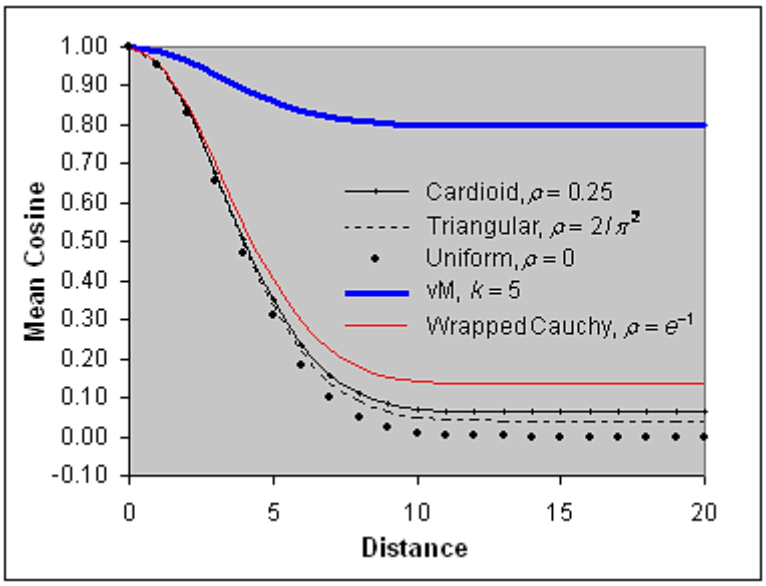

Figure 3-10. The Gaussian Cosine Model.

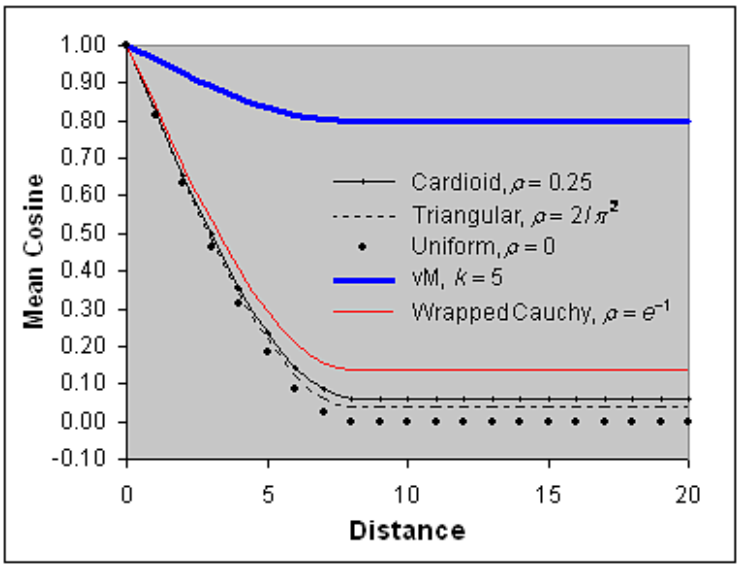

Figure 3-11. The Spherical Cosine Model.

3.6.3 The Adapted Cosine Models Are Positive Definite

Positive definiteness of the matrix of cosines is required by the circular kriging solution (Chapter 4, Section 4.3) for an optimal estimate of direction. In this subsection, it will be proven that the cosine models adapted from the positive definite covariance functions of linear kriging are positive definite. For this proof, the equivalent shifted and scaled form of the spherical cosine model in (3.14) is required.

$$\varsigma(d) \overset{(3.14)}{=} \begin{cases} 1, d = 0 \\ 1 - n_g - (1 - n_g - \rho^2)\left(\frac{3}{2}[d/r] - \frac{1}{2}[d/r]^3\right), & 0 < d < r \\ \rho^2, \quad d \geq r \end{cases}$$

$$= \begin{cases} 1, d = 0 \\ \rho^2 + (1 - n_g - \rho^2) - (1 - n_g - \rho^2)\left(\frac{3}{2}[d/r] - \frac{1}{2}[d/r]^3\right), & 0 < d < r \\ \rho^2, \quad d \geq r \end{cases}$$

$$= \begin{cases} 1, d = 0 \\ \rho^2 + (1 - n_g - \rho^2)\left(1 - \left(\frac{3}{2}[d/r] - \frac{1}{2}[d/r]^3\right)\right), & 0 < d < r \Rightarrow \\ \rho^2, \quad d \geq r \end{cases}$$

$$\varsigma(d) = \begin{cases} 1, d = 0 \\ \rho^2 + (1 - n_g - \rho^2)\left(1 - \left(\frac{3}{2}[d/r] - \frac{1}{2}[d/r]^3\right)\right), & 0 < d < r \\ \rho^2, \quad d \geq r \end{cases} \tag{3.15}$$

With $d_{ij} = d_{ji}$ the spatial distance between locations of observations *i* and *j*, let $f(d_{ij}) = a_{ij}$ be a positive definite function of distance, i.e., a covariance function of linear kriging. Then, with k_1 and k_2 constants, the cosine models structured such as (3.12), (3.13), and (3.15) can be expressed as $k_1 + k_2 f(d_{ij})$ with $k_1 = \rho^2$ and $k_2 = (1 - n_g - \rho^2)$. The circular uniform distribution has $\rho = 0$, which is the minimum mean resultant vector

length parameter of all circular distributions. The degenerate distribution has $\rho = 1$, which is the theoretical maximum. For CRV, the range of ρ^2 is $0 \le \rho^2 < 1 \Rightarrow 0 \le k_1 < 1$.

$k_2 = (1 - n_g - \rho^2)$ is the multiplier of the covariance function in (3.12), (3.13), and (3.15). $k_2 = (1 - n_g - \rho^2) = (1 - n_g) - \rho^2$ is the change in the mean cosine from the sill to the nugget. If spatial correlation does not exist, i.e., there is a "pure nugget," $k_2 = (1 - n_g) - \rho^2 = 0$, and the mean cosine vs. distance is flat. If spatial correlation exists, $k_2 = (1 - n_g) - \rho^2 > 0$. When distance $d = 0$, k_2 is increased to $1 - \rho^2$ because the nugget $n_g = 0$ when $d = 0$. A nonzero nugget applies at distances $d > 0$.

With n the number of observations and $\boldsymbol{J}$ the square n x n matrix of element 1, the n x n matrix of cosines $\boldsymbol{C}$, resulting from the element-wise application of a cosine model of the form $k_1 + k_2 f(d_{ij})$ to the matrix of pairwise distances is

$$
\begin{aligned}
\boldsymbol{C} &= \begin{bmatrix} k_1 + k_2 f(d_{11}) & k_1 + k_2 f(d_{12}) & \cdots & k_1 + k_2 f(d_{1n}) \\ k_1 + k_2 f(d_{12}) & k_1 + k_2 f(d_{22}) & \cdots & k_1 + k_2 f(d_{2n}) \\ \vdots & \vdots & \vdots & \vdots \\ k_1 + k_2 f(d_{1n}) & k_1 + k_2 f(d_{2n}) & \cdots & k_1 + k_2 f(d_{nn}) \end{bmatrix} \\
&= \begin{bmatrix} k_1 & k_1 & \cdots & k_1 \\ k_1 & k_1 & \cdots & k_1 \\ \vdots & \vdots & \vdots & \vdots \\ k_1 & k_1 & \cdots & k_1 \end{bmatrix} + k_2 \begin{bmatrix} f(d_{11}) & f(d_{12}) & \cdots & f(d_{1n}) \\ f(d_{12}) & f(d_{22}) & \cdots & f(d_{2n}) \\ \vdots & \vdots & \vdots & \vdots \\ f(d_{1n}) & f(d_{2n}) & \cdots & f(d_{nn}) \end{bmatrix} \\
&= k_1 \begin{bmatrix} 1 & 1 & \cdots & 1 \\ 1 & 1 & \cdots & 1 \\ \vdots & \vdots & \vdots & \vdots \\ 1 & 1 & \cdots & 1 \end{bmatrix} + k_2 \begin{bmatrix} a_{11} & a_{12} & \cdots & a_{1n} \\ a_{12} & a_{22} & \cdots & a_{2n} \\ \vdots & \vdots & \vdots & \vdots \\ a_{1n} & a_{2n} & \cdots & a_{nn} \end{bmatrix} \\
&= k_1 \boldsymbol{J} + k_2 \boldsymbol{A}.
\end{aligned}
$$

Now it will be proven that the matrix $\boldsymbol{C}$ is positive definite with $\boldsymbol{y}$ any n-element non zero vector.

$$
\begin{aligned}
\boldsymbol{y}^T\boldsymbol{C}\boldsymbol{y} &= \boldsymbol{y}^T(k_1\boldsymbol{J} + k_2\boldsymbol{A})\boldsymbol{y} = \boldsymbol{y}^T k_1\boldsymbol{J}\boldsymbol{y} + \boldsymbol{y}^T k_2\boldsymbol{A}\boldsymbol{y} \\
&= k_1\boldsymbol{y}^T \underbrace{\begin{bmatrix} 1_{11} & \cdots & 1_{1n} \\ \vdots & \ddots & \vdots \\ 1_{n1} & \cdots & 1_{nn} \end{bmatrix}}_{\boldsymbol{J}} \boldsymbol{y} + k_2\boldsymbol{y}^T\boldsymbol{A}\boldsymbol{y} \\
&= k_1 \left[\underbrace{\sum_{i=1}^n y_i \quad \cdots \quad \sum_{i=1}^n y_i}_{\sum \text{ for each column of } \boldsymbol{J}} \right] \boldsymbol{y} + k_2\boldsymbol{y}^T\boldsymbol{A}\boldsymbol{y} \\
&= k_1\left(y_1\left[\sum_{i=1}^n y_i\right] + y_2\left[\sum_{i=1}^n y_i\right] + \cdots + y_n\left[\sum_{i=1}^n y_i\right)\right) + k_2\boldsymbol{y}^T\boldsymbol{A}\boldsymbol{y} = \\
&= k_1(y_1 + y_2 + \cdots + y_n)\left[\sum_{i=1}^n y_i\right] + k_2\boldsymbol{y}^T\boldsymbol{A}\boldsymbol{y} \\
&= k_1\left[\sum_{i=1}^n y_i\right]\left[\sum_{i=1}^n y_i\right] + k_2\boldsymbol{y}^T\boldsymbol{A}\boldsymbol{y} \\
&= \underbrace{k_1}_{0\le k_1<1} \underbrace{\left[\sum_{i=1}^n y_i\right]^2}_{\ge 0} + \underbrace{k_2}_{>0} \underbrace{\boldsymbol{y}^T\boldsymbol{A}\boldsymbol{y}}_{\boldsymbol{A}\text{ P. D.}\Rightarrow >0} \\
&> 0 \Rightarrow \\
\boldsymbol{y}^T\boldsymbol{C}\boldsymbol{y} &> 0 \ \forall \boldsymbol{y} \neq \boldsymbol{0}
\end{aligned}
$$

Hence, $\boldsymbol{C}$ is positive definite by Appendix B, Section B.2, point 3.

3.7 Cosineogram of Ocean Wind in a South Polar Region

In this section, circular-spatial correlation will be extracted from ocean wind of a south polar region. A model was computed for longitude 69.5º E to 109.5º E by latitude -59.5º N to -40.5º N in 1º increments by averaging the data of Chapter 2, Subsection 2.2.1 via R package CircSpatial function CircDataimage (Chapter 2, and Appendices J.10 and K.2) with input as in Appendix J, Subsection J.10.6, step 1, and smoothing the averages with bandwidth 2.5º in the plane of longitude and latitude (J.10.6, step 8). The smoothed average directions from CircDataimage were output to the R workspace in the list object CircDataimageGlobals. Appendix L, Section L.2 shows usage of the elements of CircDataimageGlobals. Figure 3-12 shows the image of this model. The spatial correlation is expressed in the cosineocloud and cosineogram in Figure 3-13. The cosineocloud (grey points) is here defined as the plot of the cosines of the angles

between all pairs of directions vs. distance between measurement locations. The cosineocloud is useful for examination of the individual cosines. The cosineogram (red curve) as defined in Section 3.2, reduces the cosineocloud to the plot of the mean cosine vs. distance. Between distances of 0 and 1 on the horizontal axis, spatial correlation is changing rapidly. At a distance of about 3.8, the mean cosine tends to be constant at about 0.45 indicating that direction is not correlated. Hence, the range is 3.8 and the sill is 0.45. Circular kriging, as described in Chapter 4, requires a cosine model which is smooth, continuous, and positive definite. The shape of the cosineogram in Figure 3-13 suggests the exponential cosine model in (3.12), which is overplotted as a blue dashed curve over the full range of distances for comparison with the empirical cosineogram. The fit of the model to the cosineogram is adequate. The exponential cosine model characterizes the circular-spatial correlation in this region of ocean wind data as asymptotic, but without the inflexion (S shape) of the gaussian cosine model. The exponential cosine model is fairly linear near the origin and falls to the sill much more quickly than the spherical cosine model.

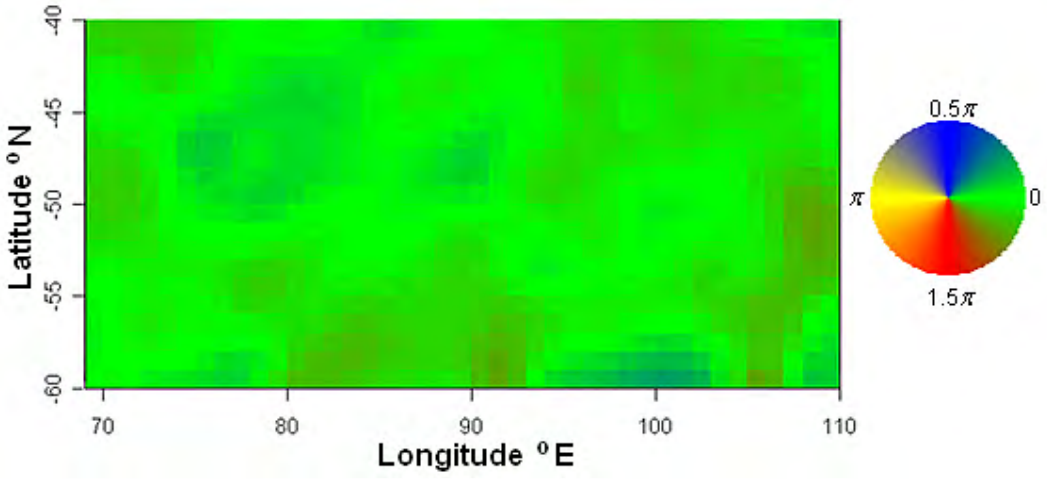

Figure 3-12. Circular Dataimage of Model of Ocean Wind Direction for South Polar Region. Direction, which is coded by the color wheel, is relatively homogeneous and varies about the direction of 0 radians.

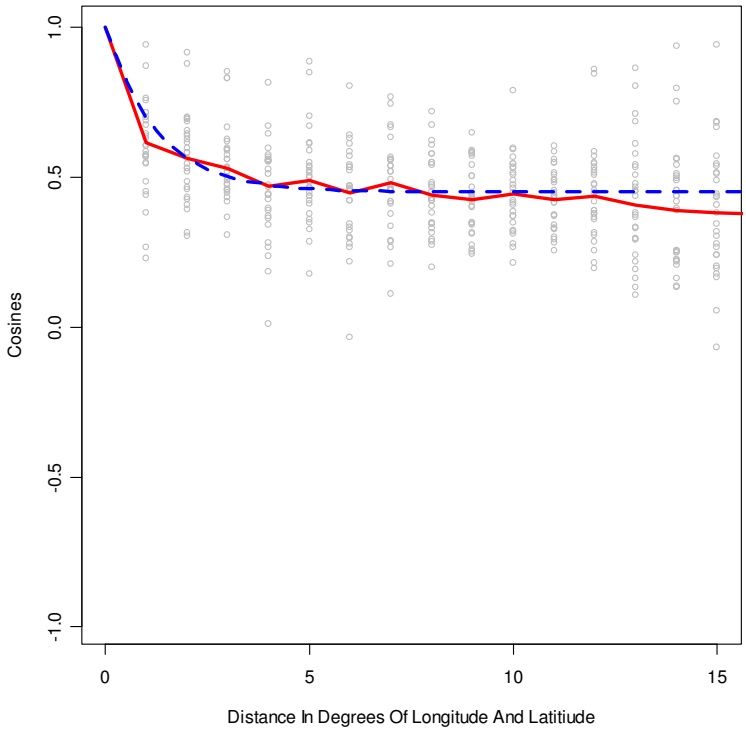

Figure 3-13. Cosineocloud, Cosineogram, and Exponential Model of South Polar Ocean Wind. The cosineocloud (grey points) shows the cosines of the angles between all pairs of directions vs. distance between measurement locations. The cosineogram (red solid curve) reduces the cosineocloud to the plot of the mean cosine vs. distance. The sill (plateau), where the random components of direction are uncorrelated, occurs at a distance of about 3.8 at a mean cosine of about 0.45. The exponential model (blue dashed curve) is overplotted for comparison.

3.8 Chapter Summary and Future Work

In this chapter, we discussed the cosineocloud, the empirical cosineogram, and theoretical cosine models. The cosineogram plots the empirical spatial correlation in circular-spatial data as the mean cosine of the angle between random components of direction at locations vs. distance d between observation locations. With $\hat{\varsigma}(d)$ the mean cosine, $\boldsymbol{x}_i$ and $\boldsymbol{x}_j$ vectors of location coordinates of observations i and j, respectively, $\| \boldsymbol{x}_j - \boldsymbol{x}_i \|$ the linear distance between locations of observations i and j, and $N(d)$ the number of pairs of observations of direction separated by a distance within a tolerance

ε of *d,* the cosineogram is a plot of $\hat{\varsigma}(d) = {}^{1}\!/_{N(d)} \sum_{\left| \| \boldsymbol{x}_j - \boldsymbol{x}_i \| - d \right| < \varepsilon} \cos(\theta_j - \theta_i)$ vs. *d*. For an example, a cosineogram was constructed from homogeneous ocean wind data in a south polar region.

The cosine model fitted to the cosineogram characterizes the spatial correlation in a form useful for circular kriging.

- The mean cosine equals 1 at zero distance.
- The mean cosine at distances close to 0 may be reduced by measurement error. This reduction n_g is called the nugget effect.
- The range *r* is a scale parameter. The range of the spherical cosine model is the distance beyond which CRV are uncorrelated.
- The sill is the mean cosine at distances where CRV are uncorrelated. The theoretical sill is ρ^2.

The theoretical sill was derived as the square of the mean resultant vector length of the circular probability distribution underlying the circular-spatial data. For the circular probability distributions cardioid, triangular, uniform $(\rho = 0)$, von Mises, and wrapped Cauchy, the mean resultant vector length equals the parameter ρ of the underlying circular probability distribution. The theoretical sill was verified by simulation.

Introductory cosine models, which are required for circular kriging, were adapted from the exponential, Gaussian, and spherical covariance functions used for linear kriging by shifting and scaling the covariance function. With *d* the distance between measurement locations, ρ the mean vector resultant length parameter of the circular probability distribution, $0 \le \rho < 1$, n_g the nugget, $0 \le n_g < 1 - \rho^2$, *r* the range, and c(*d, r*) the covariance function from linear kriging with a maximum of 1,

the general form of the cosine model is

$$\varsigma(d)=\begin{cases}1, d=0\\ \rho^2+\left(1-n_g-\rho^2\right)c(d,r), d>0.\end{cases}$$

This form was proven to produce a positive definite cosine matrix.

Future work includes the development of theoretical foundations of directional cosineograms for anisotropic circular-spatial data where the range varies with the geographic direction.